

498
11/10/80 T.S

SAN-3042-3

12/1986

AMORPHOUS SILICON SOLAR CELLS BY HYDROGEN IMPLANTATION

Quarterly Report No. 3 for Period July 1–September 30, 1979

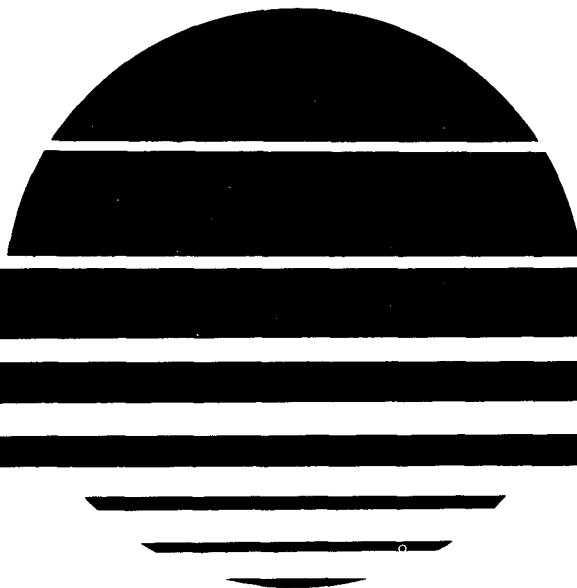
MASTER

By
A. R. Kirkpatrick
A. A. Melas

January 1980

Work Performed Under Contract No. AC03-79ET 23042

Spire Corporation
Bedford, Massachusetts



U.S. Department of Energy



Solar Energy

DISCLAIMER

This report was prepared as an account of work sponsored by an agency of the United States Government. Neither the United States Government nor any agency thereof, nor any of their employees, makes any warranty, express or implied, or assumes any legal liability or responsibility for the accuracy, completeness, or usefulness of any information, apparatus, product, or process disclosed, or represents that its use would not infringe privately owned rights. Reference herein to any specific commercial product, process, or service by trade name, trademark, manufacturer, or otherwise does not necessarily constitute or imply its endorsement, recommendation, or favoring by the United States Government or any agency thereof. The views and opinions of authors expressed herein do not necessarily state or reflect those of the United States Government or any agency thereof.

DISCLAIMER

Portions of this document may be illegible in electronic image products. Images are produced from the best available original document.

**AMORPHOUS SILICON SOLAR CELLS
BY HYDROGEN IMPLANTATION**

**QUARTERLY REPORT NO. 3
FOR THE PERIOD
1 JULY - 30 SEPTEMBER 1979**

A.R. Kirkpatrick and A.A. Melas

January 1980

**SPIRE CORPORATION
PATRIOTS PARK
BEDFORD, MA 01730**

Prepared for the

**U.S. DEPARTMENT OF ENERGY
SOLAR ENERGY
Under Contract No. 03-79-ET-23042.000**

m/s
DISTRIBUTION OF THIS DOCUMENT IS UNLIMITED



TABLE OF CONTENTS

| <u>Section</u> | | <u>Page</u> |
|----------------|---|-------------|
| 1 | INTRODUCTION | 1 |
| 2 | PROGRAM DISCUSSION | 2 |
| | 2.1 Program Plan | 2 |
| | 2.2 Investigation of Implantation/Annealing Effects | 15 |
| | 2.3 Material Evaluations | 22 |
| 3 | SUMMARY | 22 |
| | REFERENCES | 23 |

LIST OF FIGURES

| <u>Figure</u> | <u>Page</u> |
|--|-------------|
| 1 AM0 I-V Curves for Cell Device No. 2150-6-7 | 4 |
| 2 AM0 I-V Curves for Cell Device No. 2150-8-8 | 5 |
| 3 AM0 I-V Curves for Cell Device No. 2150-29-2 | 6 |
| 4 AM0 I-V Curves for Cell Device No. 2150-26-7 | 7 |
| 5 Effect of $^{1}\text{H}^{+}$ and $^{28}\text{Si}^{+}$ Implants on Transmittance of Silicon Film Samples | 9 |
| 6 $^{28}\text{Si}^{+}$ Implants Used for Amorphization of Polysilicon Film | 10 |
| 7 Anticipated Distribution of Hydrogen in Silicon From Combined 10, 20 and 50 keV Proton Implants | 13 |
| 8 AM0 I-V Curves for Cell Device No. 2269-15-4 | 14 |
| 9 Absorption Coefficient for Material Unit B-11 After Si^{+} Implantation | 17 |
| 10 Infrared Absorption Spectrum for Device Unit No. 2191-13 After $3.3 \times 10^{17} \text{ H}^{+}/\text{cm}^2$ Implant | 18 |
| 11 Infrared Absorption Spectrum for Device Unit No. 2150-19 After: <ol style="list-style-type: none"> 1. $3 \times 10^{15} \text{ /cm}^2$ $^{28}\text{Si}^{+}$ Implant 2. $5.3 \times 10^{17} \text{ /cm}^2$ $^{1}\text{H}^{+}$ Implant 3. 24 Hr Anneal at 250°C 4. 30 Min Anneal at 300°C | 19 |
| 12 Infrared Absorption Spectrum for Material Unit No. B-11 After $^{28}\text{Si}^{+}$ Implant ($8 \times 10^{15} \text{ /cm}^2$) and $5 \times 10^{17} \text{ H}^{+}/\text{cm}^2$ Implant | 20 |

SECTION 1

INTRODUCTION

Ion implantation can be an effective means of introducing virtually any constituent atom into a surface to a depth of usually 1 micron or less. The process involves high-energy particle impact which results in microscopic disordering of the area affected and can be employed for amorphization purposes. It is also possible to change the chemical composition of the implanted area in a controlled and reproducible manner. The purpose of this program for the investigation of "Amorphous Silicon Solar Cells by Hydrogen Implantation" is to examine applications of ion implantation in the fabrication of amorphous silicon solar cells.

This program utilizes ion implantation to alter the properties of a polycrystalline silicon thin film deposited by chemical vapor deposition in the following ways:

1. To amorphize using $^{28}\text{Si}^+$ or $^{40}\text{Ar}^+$
2. To hydrogenate with $^1\text{H}^+$
3. To dope with $^{31}\text{P}^+$ or $^{11}\text{B}^+$
4. To introduce other elements that can improve photovoltaic properties of already amorphized material, such as $^{19}\text{F}^+$ or $^{16}\text{O}^+$.

Two types of study structures are used; first a device structure consisting of nine individual 0.1 cm^2 solar cells and second the material structure which is $2 \times 2 \text{ cm}$. Both types of structures are processed in the same way and thus the effect of an individual process step is assessed both at the solar cell and at the material level. Useful correlations between the material and photovoltaic properties are thus possible without delay.

SECTION 2

PROGRAM DISCUSSION

2.1 PROGRAM PLAN

This 12 month program involves the following:

| | |
|--|------------|
| 1. Development of Special Implantation/ Annealing Facilities and Procedures | Months 1-4 |
| 2. Development of Amorphous Silicon Solar Cell and Material Test Structures | 2-4 |
| 3. Preliminary Survey of Ion Implantation Effects Upon Device Performance | 5-7 |
| 4. Demonstration of an Amorphous Silicon Solar Cell | 6-9 |
| 5. Investigation to Improve Amorphous Silicon Material | 8-10 |
| 6. Investigation to Improve Amorphous Silicon Cell Performance | 8-10 |
| 7. Fabrication of Best Status Cells | 6-12 |

Work during the third quarter of this program included the following activities:

- Evaluation of $^1H^+$ and $^{28}Si^+$ implantation effects on completed devices
- Demonstration of a functioning amorphous silicon solar cell
- Investigation to improve the performance of amorphous silicon solar cells and material properties
- Evaluation of characteristics of amorphous silicon prepared using ion implantation

Two ion implanters at Spire are being used for this program and all ions of interest are available at beam currents of a few hundred microamperes and energies from 10 through 200 keV. Very high level doses of hydrogen at multiple energies are being used to saturate dangling bonds and to hydrogenate up to 1 micron of material.

The use of solar cell devices and solar cell measurements are emphasized in this program. This way the effect of each implantation step can be assessed individually. During the period of July through September the emphasis was on the preparation of polysilicon devices and subsequent implantation matrix studies. Device and material improvements through annealing were investigated. Also, preliminary material investigations were initiated.

2.2 INVESTIGATION OF IMPLANTATION/ANNEALING EFFECTS

The investigation of the effects on device performance of the various implanted ions and annealing procedures can be divided as follows:

- Effects of single-ion implantations with or without annealing
- Effects of combined-ion implantation
- Effects of combined-ion implantation followed by annealing

In the first category $^1H^+$ and $^{28}Si^+$ implants were investigated. Thermal processing in the temperature range from $100^{\circ}C$ to $250^{\circ}C$ and pulsed electron beam annealing at a fluence level of 0.1 cal/cm^2 were examined. Various effects were monitored by the changes in the AM0 I-V curves in the device structures and by the changes in the transmittance versus wavelength in the material structures. In the second category both $^1H^+$ and $^{28}Si^+$ were used in various sequences, dose levels and energies. The effects were again monitored in the same manner. Finally in the third category both $^1H^+$ and $^{28}Si^+$ were implanted and annealed at $250^{\circ}C$ and at $300^{\circ}C$. Figures 1-4 show the effects of H^+ implantation at a dose of $1 \times 10^{17} H^+/\text{cm}^2$ and 50 keV energy on the AM0 I-V curve and the subsequent thermal treatment. The device structure is $2 \times 2 \text{ cm}^2$ and consists of 9 individual cells each 0.1 cm^2 in area and separated by 0.1 microns thick thermal oxide. The entire device structure was illuminated during the AM0 I-V measurement of the individual cells. The material structures are $2 \times 2 \text{ cm}^2$ fused silica slides coated with 1.5 microns of CVD polycrystalline silicon. Four temperatures were tried, $100^{\circ}C$, $150^{\circ}C$, $200^{\circ}C$ and $250^{\circ}C$. A larger device performance recovery is

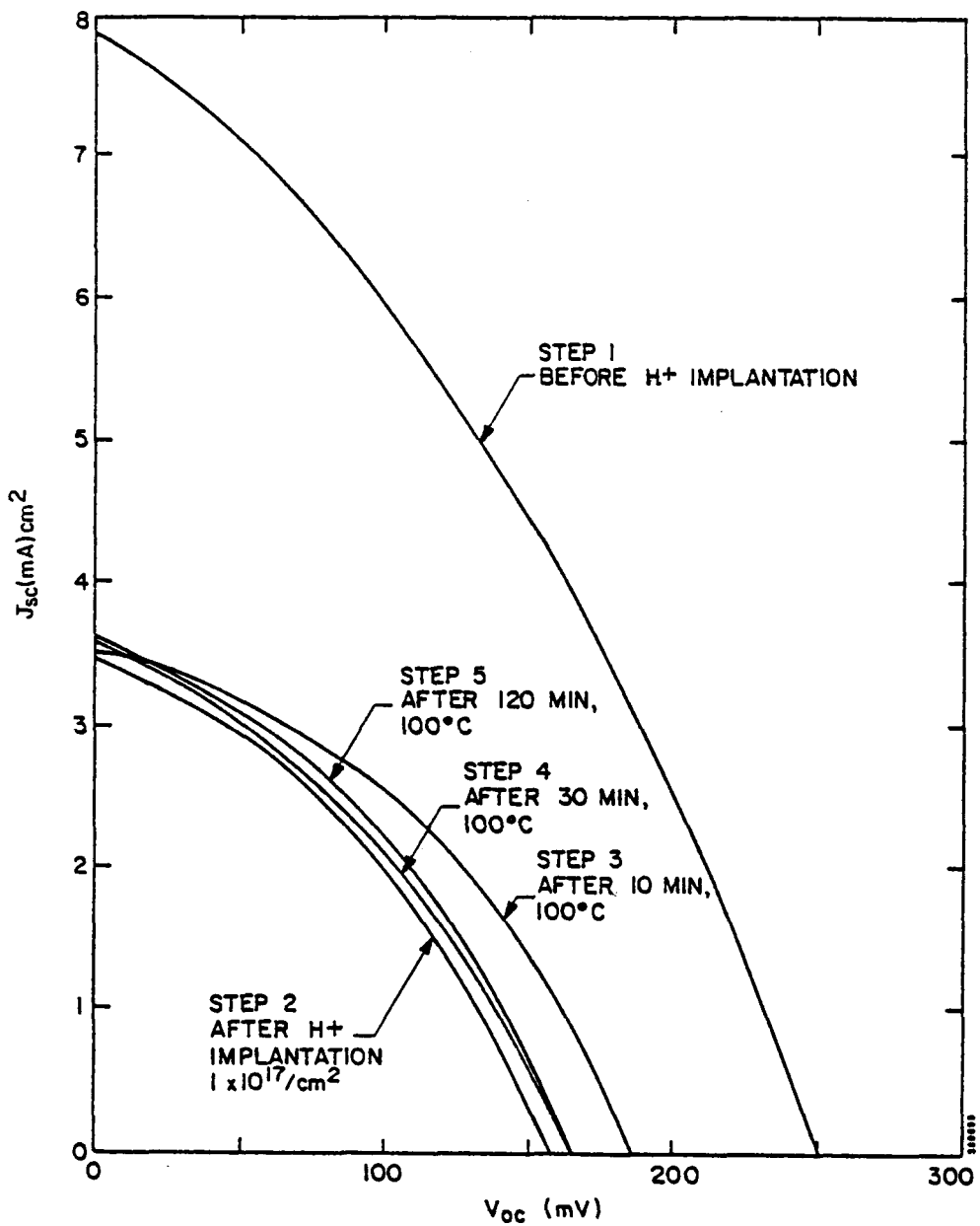


FIGURE 1. AM0 I-V CURVES FOR CELL DEVICE NO. 2150-6-7

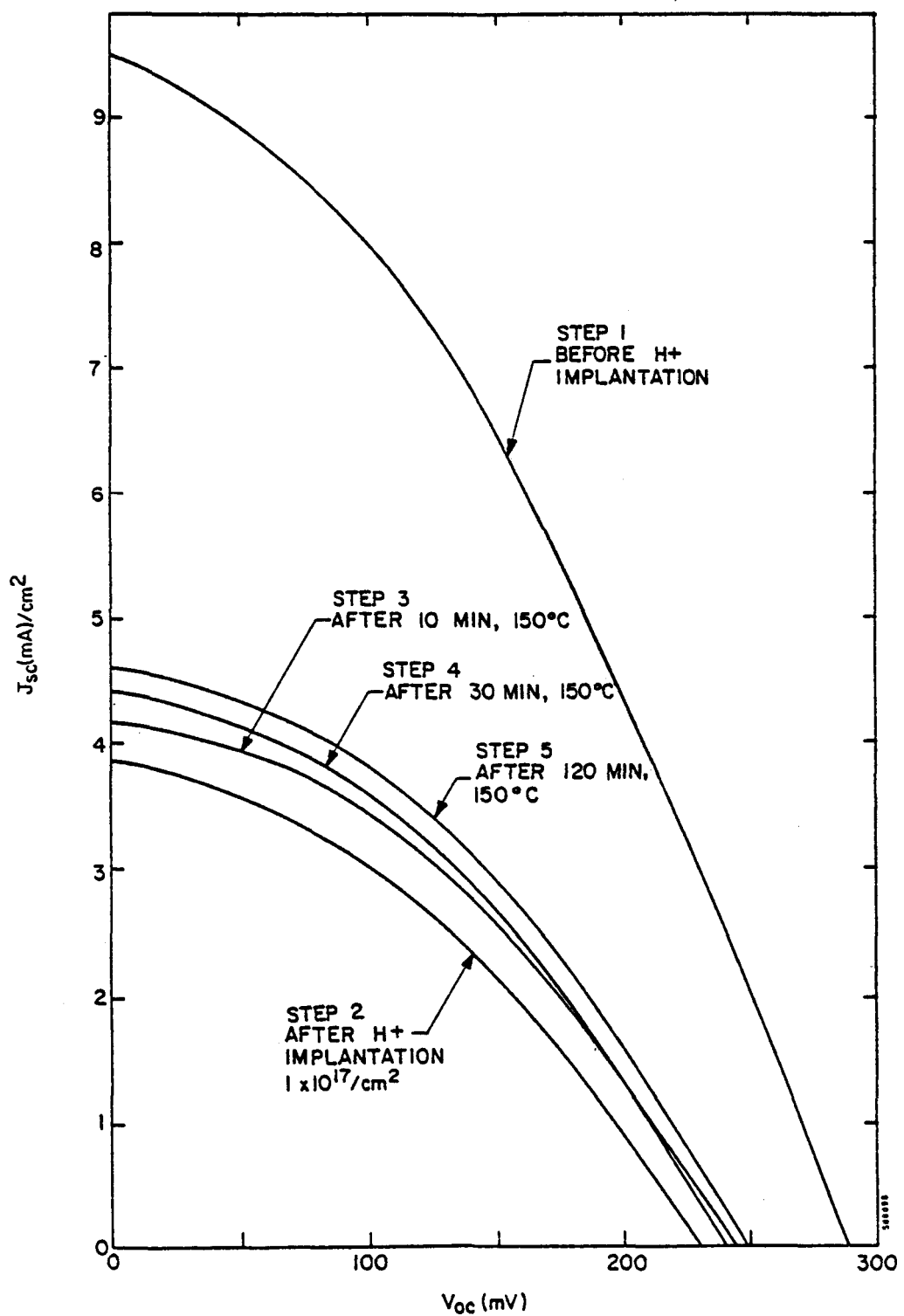


FIGURE 2. AM0 I-V CURVES FOR CELL DEVICE-NO. 2150-8-8

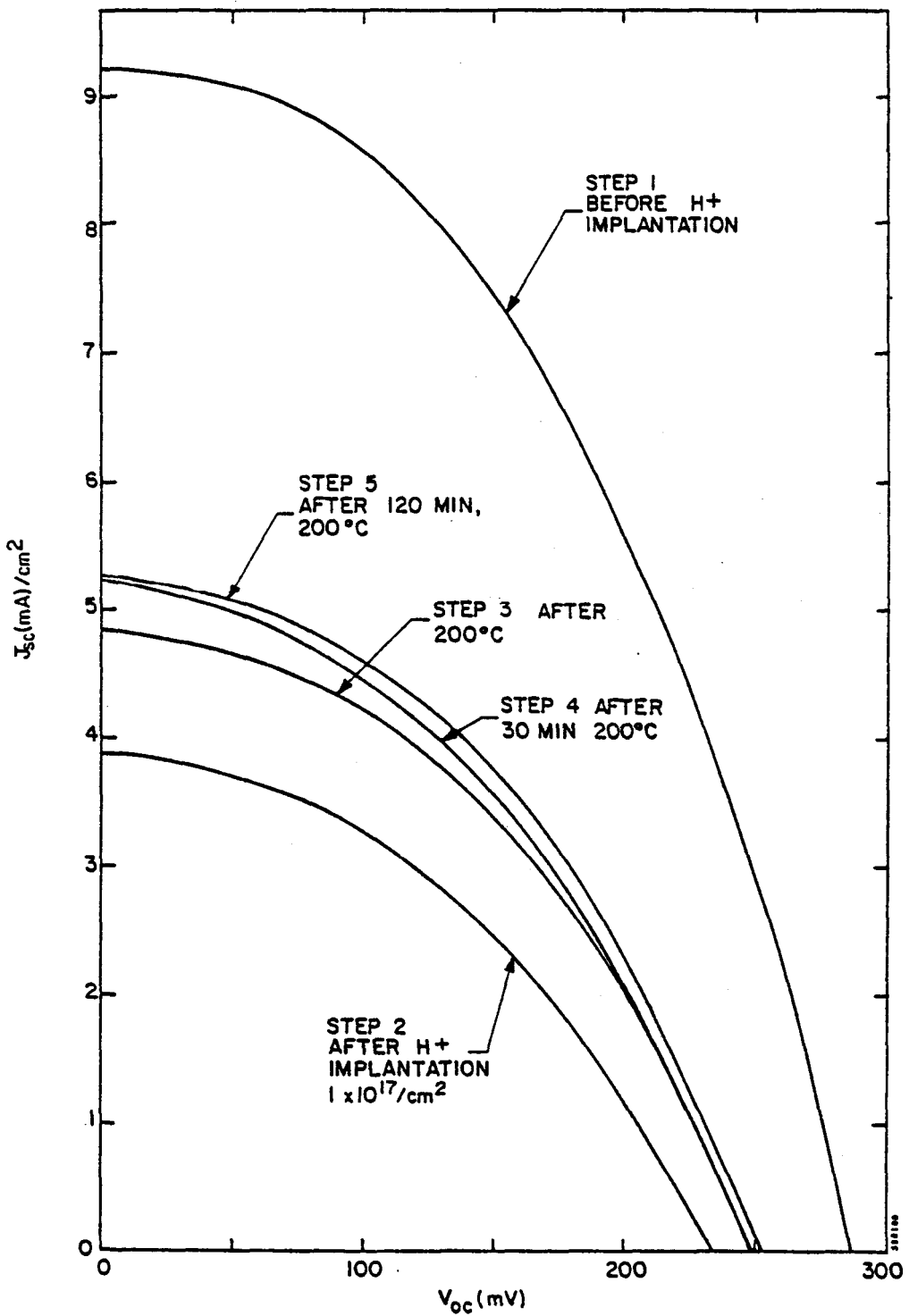


FIGURE 3. AM0 I-V CURVES FOR CELL DEVICE NO. 2150-29-2

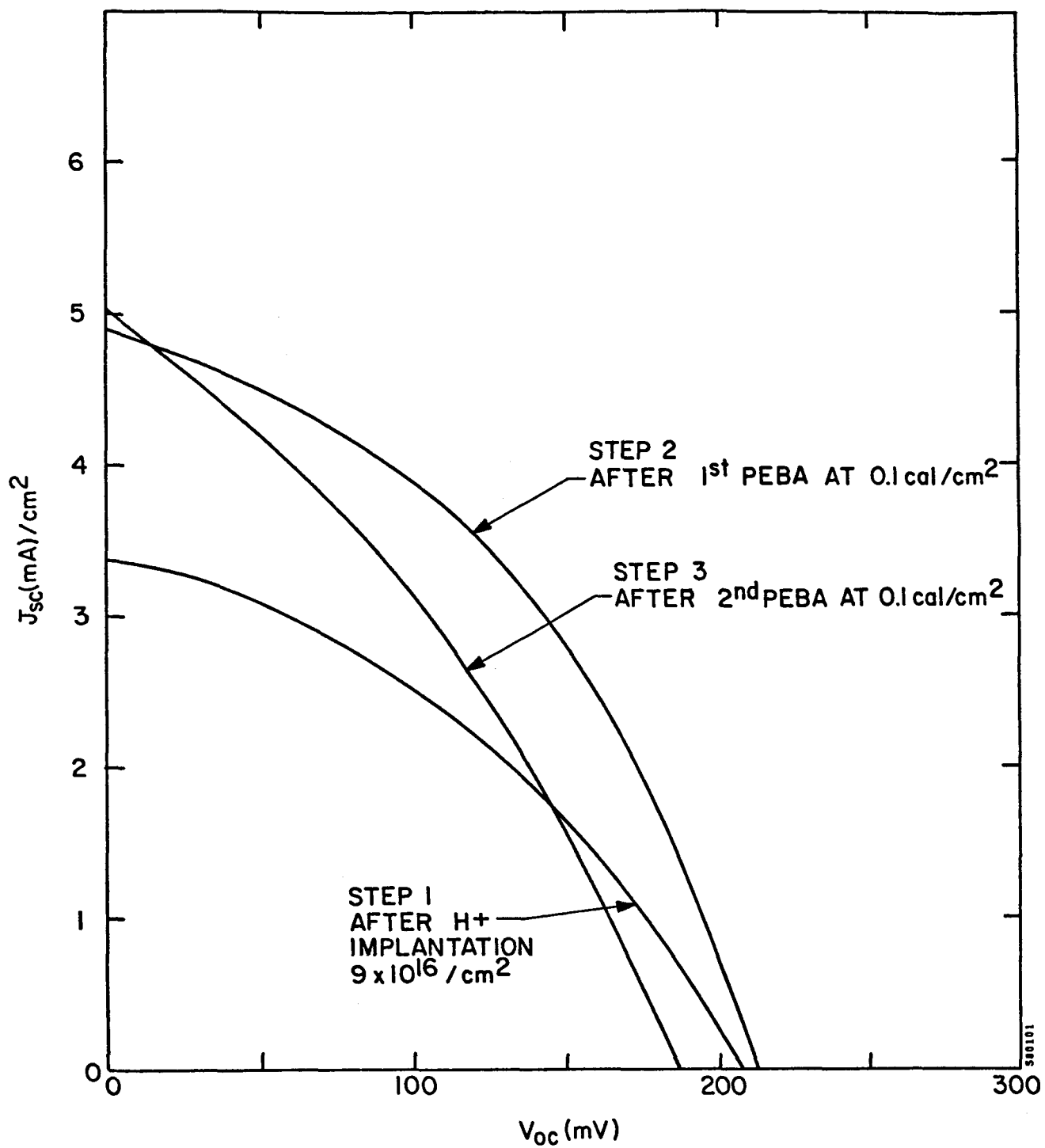


FIGURE 4. AM0 I-V CURVES FOR CELL DEVICE NO. 2150-26-7

observed with increasing temperature. Figure 5 shows the effect of H^+ and Si^+ implantation on the percent transmittance of visible light versus wavelength.

Generally a higher dose of implanted H^+ increases absorptance and the thermal processing increases transmittance.

The $Si^{28}+$ implantation at a total dose of $8 \times 10^{15} Si^+/cm^2$ is done in the following manner and as reported in the literature⁽¹⁾:

- With very low total beam current, 7-10 microamperes
- At four energy levels:
 - (a) 200 keV, $3 \times 10^{15} /cm^2$
 - (b) 150 keV, $2 \times 10^{15} /cm^2$
 - (c) 100 keV, $2 \times 10^{15} /cm^2$
 - (d) 50 keV, $1 \times 10^{15} /cm^2$

The combined effect of these implantations is shown in Figure 6, which indicates a disordered layer of 4500\AA . As expected, a severe degradation in cell device performance is observed. On the other hand, transmittance is decreased substantially as shown in Figure 5. Again thermal processing or pulsed electron beam annealing serve to reduce absorbance in the optical region, but the device performance recovers as discussed below.

Combined-ion implantation effects have received the most attention. A large number of possible sequences were tried and evaluated (see Table 1). The dose of implanted H^+ varied as well as the energy. It is necessary to overlap the implantation range of hydrogen to match the $Si^{28}+$ implanted region. For this reason a three-energy hydrogen implantation was arrived at (see Figure 7), which satisfies this requirement. The annealing temperature was $250^\circ C$ for all wafers except for those that received additional treatment at $300^\circ C$. Either nitrogen or forming gas was used for the anneals. Figure 8 shows a typical good result. The AM0 I-V curves after each processing step are compiled. The indication is that a combined $Si^{28}+$ and H^+ implantation at a high dose followed by prolonged furnace annealing at $250^\circ C$ can anneal out the implantation damage and thus improve the material photovoltaic properties. As expected there is a substantial improvement in device open-circuit voltage after this type of processing. By way of comparison a good polysilicon device, $0.1 cm^2$ in area, with V_{oc} at AM0 similar to cell no. 2269-15-4, under reduced illumination to yield the same I_{sc} , is seen to yield

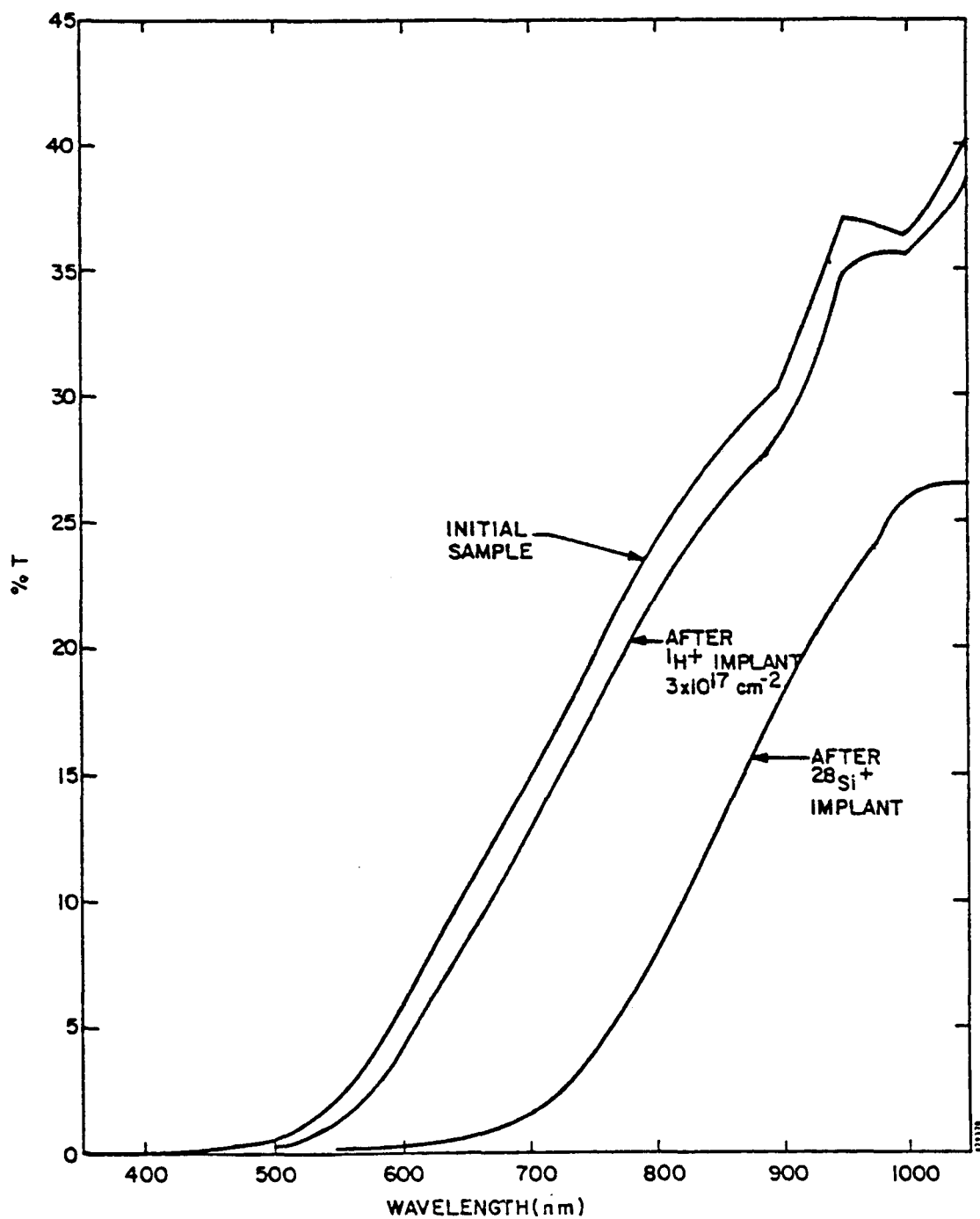


FIGURE 5. EFFECT OF $^1\text{H}^+$ AND $^{28}\text{Si}^+$ IMPLANTS ON TRANSMITTANCE OF SILICON FILM SAMPLES

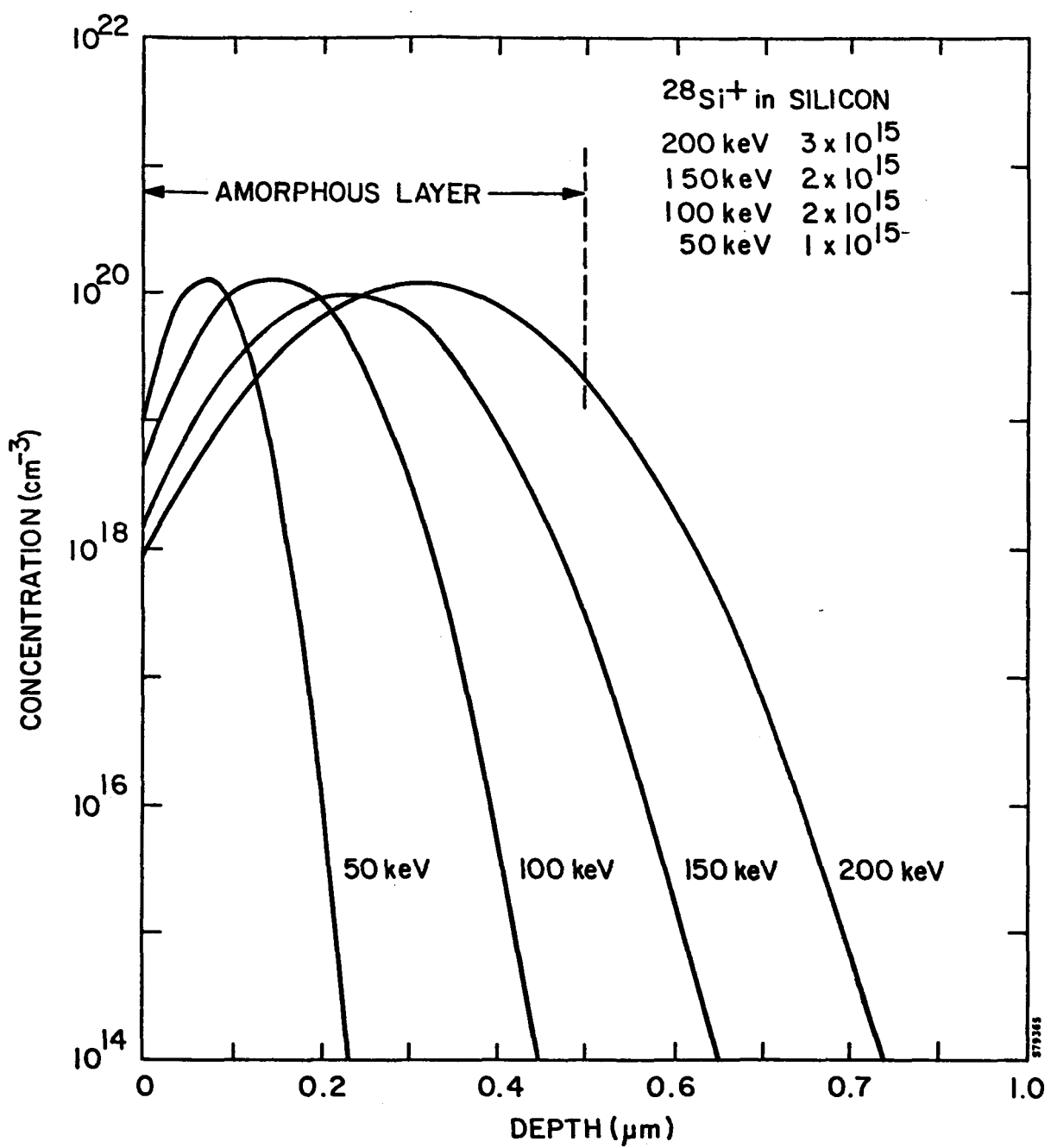


FIGURE 6. $^{28}\text{Si}^+$ IMPLANTS USED FOR AMORPHIZATION OF POLYSILICON FILM

TABLE 1. MATRIX IMPLANTATIONS EVALUATED

| Species Used (Energy + Dose) | | Thermal Treatment (Temperature + Time) |
|---------------------------------|---|---|
| 1 | $1 \times 10^{16} \text{ } \text{H}^+/\text{cm}^2$, 50 keV | 100°C 150°C 2 hr total 200°C 250°C |
| 2 | $1 \times 10^{17} \text{ } \text{H}^+/\text{cm}^2$, 50 keV | same as above |
| 3A | i. $1 \times 10^{16} \text{ } \text{H}^+/\text{cm}^2$, 50 keV ii. $2 \times 10^{15} \text{ } \text{Si}^+/\text{cm}^2$, 200 keV $1 \times 10^{15} \text{ } \text{Si}^+/\text{cm}^2$, 80 keV | 250°C , 2 hr |
| 3B | i. $1 \times 10^{17} \text{ } \text{H}^+/\text{cm}^2$, 50 keV ii. $2 \times 10^{15} \text{ } \text{Si}^+/\text{cm}^2$, 200 keV $1 \times 10^{15} \text{ } \text{Si}^+/\text{cm}^2$, 80 keV | same as above |
| 4A | i. $2 \times 10^{15} \text{ } \text{Si}^+/\text{cm}^2$, 200 keV $1 \times 10^{15} \text{ } \text{Si}^+/\text{cm}^2$, 80 keV ii. $1 \times 10^{16} \text{ } \text{H}^+/\text{cm}^2$, 50 keV | same as above |
| 4B | i. $2 \times 10^{15} \text{ } \text{Si}/\text{cm}^2$, 200 keV $1 \times 10^{15} \text{ } \text{Si}/\text{cm}^2$, 80 keV ii. $1 \times 10^{17} \text{ } \text{H}^+/\text{cm}^2$, 50 keV | same as above |
| 5 | i. $1 \times 10^{16} \text{ } \text{H}^+/\text{cm}^2$, 50 keV ii. $2 \times 10^{15} \text{ } \text{Si}^+/\text{cm}^2$, 200 keV $1 \times 10^{15} \text{ } \text{Si}^+/\text{cm}^2$, 80 keV iii. $1 \times 10^{17} \text{ } \text{H}^+/\text{cm}^2$, 50 keV | same as above |

TABLE 1. MATRIX IMPLANTATIONS EVALUATED (Concluded)

| | Species Used (Energy + Dose) | Thermal Treatment (Temperature + Time) |
|---|--|---|
| 6 | i. $2 \times 10^{15} \text{ Si}^+/\text{cm}^2$, 200 keV $1 \times 10^{15} \text{ Si}^+/\text{cm}^2$, 80 keV ii. $3 \times 10^{16} \text{ H}^+/\text{cm}^2$, 50 keV iii. $3 \times 10^{17} \text{ H}^+/\text{cm}^2$, 50 keV iv. $1 \times 10^{17} \text{ H}^+/\text{cm}^2$, 25 keV v. $1 \times 10^{17} \text{ H}^+/\text{cm}^2$, 10 keV | 250°C 24 hr |
| 7 | i. $3 \times 10^{17} \text{ H}^+/\text{cm}^2$, 50 keV ii. $3 \times 10^{15} \text{ Si}^+/\text{cm}^2$, 200 keV $2 \times 10^{15} \text{ Si}^+/\text{cm}^2$, 150 keV $2 \times 10^{15} \text{ Si}^+/\text{cm}^2$, 100 keV $1 \times 10^{15} \text{ Si}^+/\text{cm}^2$, 50 keV iii. $1 \times 10^{17} \text{ H}^+/\text{cm}^2$, 25 keV iv. $1 \times 10^{17} \text{ H}^+/\text{cm}^2$, 10 keV | 250°C 24 hr |
| 8 | i. $3 \times 10^{15} \text{ Si}^+/\text{cm}^2$, 200 keV $2 \times 10^{15} \text{ Si}^+/\text{cm}^2$, 150 keV $2 \times 10^{15} \text{ Si}^+/\text{cm}^2$, 100 keV $1 \times 10^{15} \text{ Si}^+/\text{cm}^2$, 50 keV ii. $1 \times 10^{17} \text{ H}^+/\text{cm}^2$, 25 keV iii. $1 \times 10^{17} \text{ H}^+/\text{cm}^2$, 10 keV | 250°C 24 hr |
| 9 | i. $3 \times 10^{16} \text{ H}^+/\text{cm}^2$, 50 keV ii. $3 \times 10^{17} \text{ H}^+/\text{cm}^2$, 50 keV iii. $3 \times 10^{15} \text{ Si}^+/\text{cm}^2$, 200 keV $2 \times 10^{15} \text{ Si}^+/\text{cm}^2$, 150 keV $2 \times 10^{15} \text{ Si}^+/\text{cm}^2$, 100 keV $1 \times 10^{15} \text{ Si}^+/\text{cm}^2$, 50 keV iv. $1 \times 10^{17} \text{ H}^+/\text{cm}^2$, 25 keV v. $1 \times 10^{17} \text{ H}^+/\text{cm}^2$, 10 keV | 250°C 24 hr |

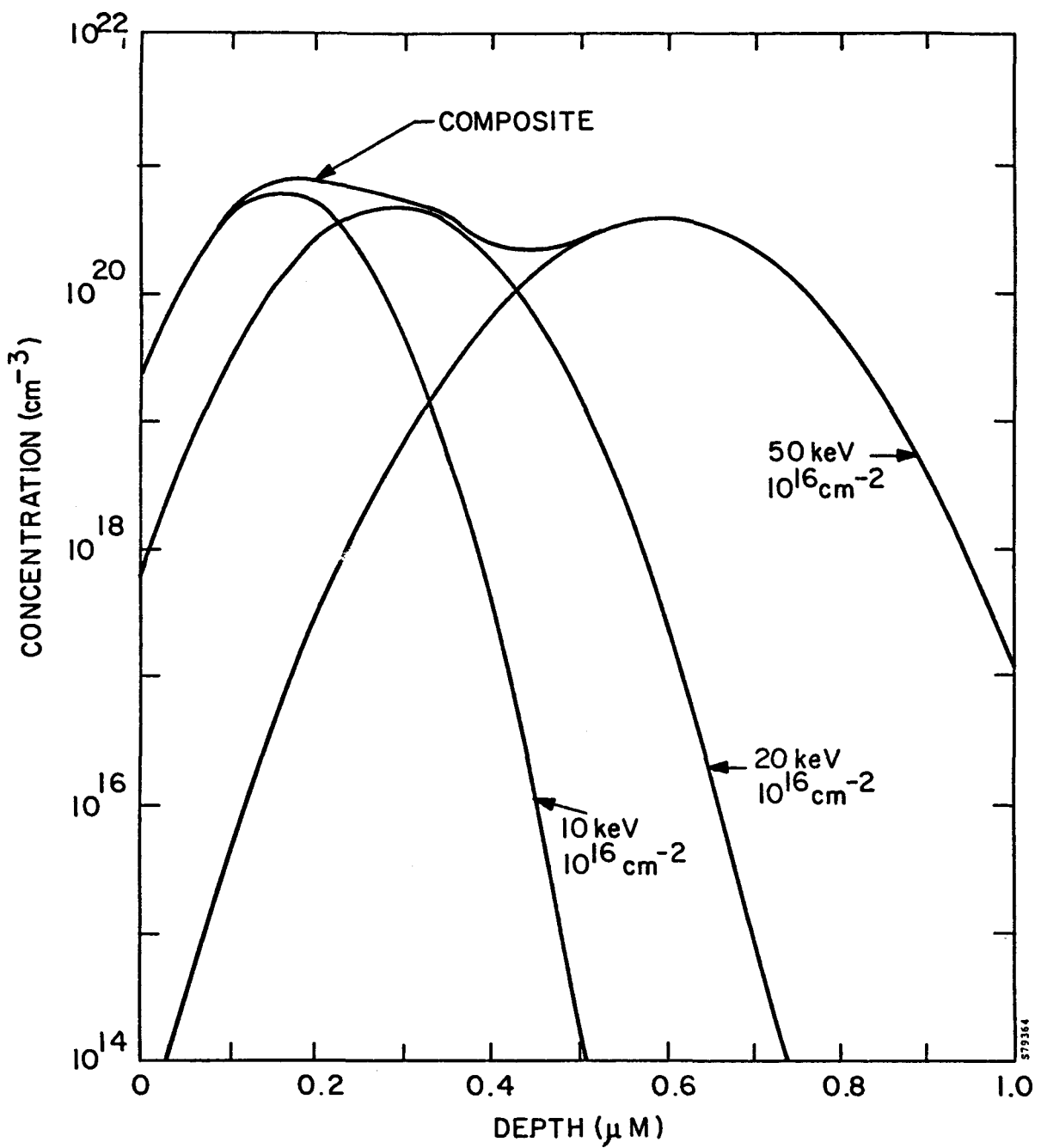


FIGURE 7. ANTICIPATED DISTRIBUTION OF HYDROGEN IN SILICON FROM COMBINED 10, 20 AND 50 keV PROTON IMPLANTS

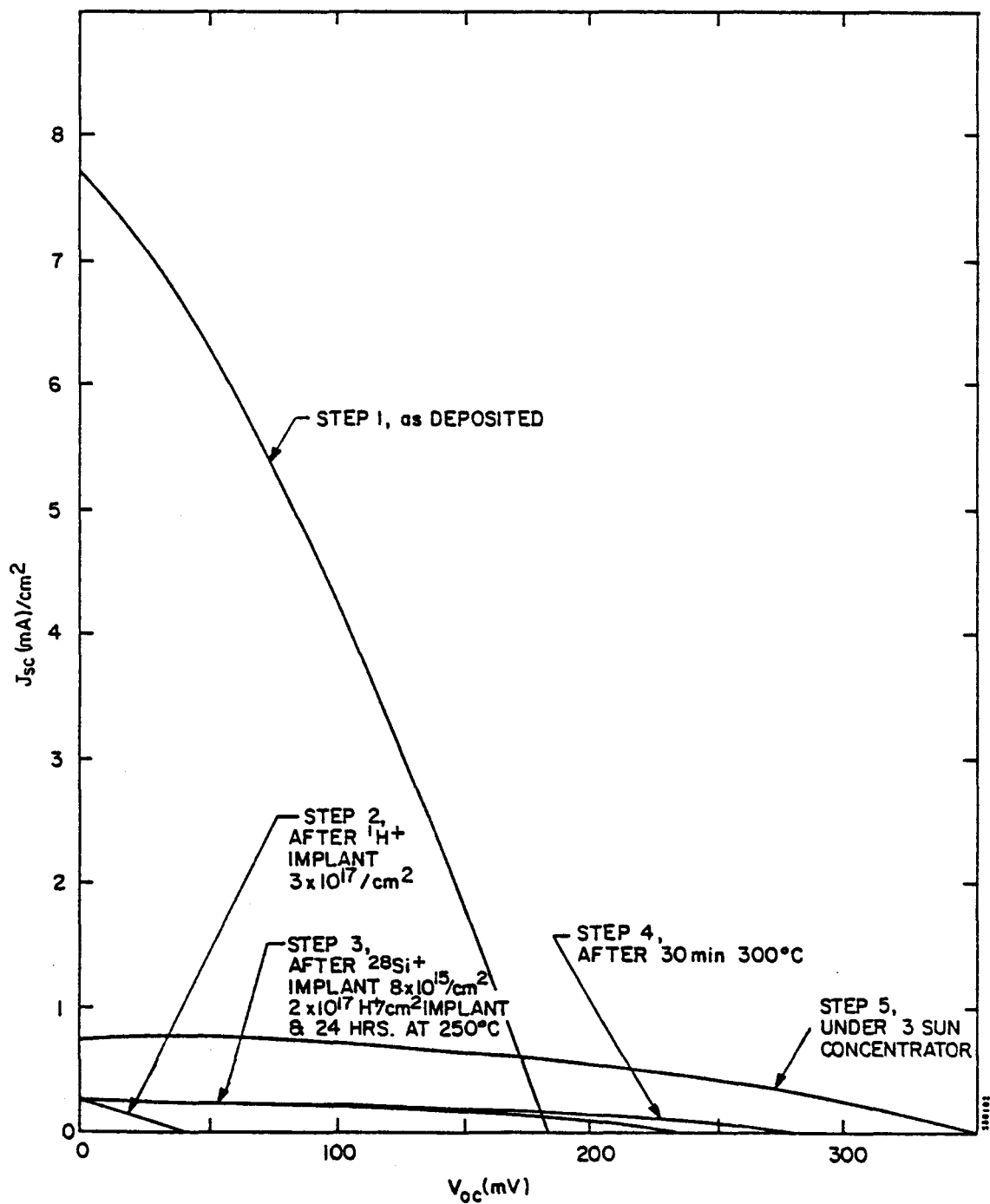


FIGURE 8. AM0 I-V CURVES FOR CELL DEVICE NO. 2269-15-4

only 63 mV. Also, a good, single-crystal-Si, 2 x 2-cm spacecraft cell made by Spire is seen to produce only 326 mV under reduced illumination to equal the I_{sc} density of cell no. 2269-15-4. Investigations will continue in a similar fashion with a liquid-nitrogen-cooled substrate during $^{28}\text{Si}^+$ implantation-amorphization. The cumulative effect of implanting $^{19}\text{F}^+$ and other ions will also be evaluated. It has been reported in the literature that the addition of fluorine to a glow-discharge, α -Si-H solar cell improves its spectral response at both ends of the visible spectrum.⁽²⁾ Spire capabilities in $^{19}\text{F}^+$ implantation are such that a high dose, such as $1 \times 10^{17}/\text{cm}^2$ can be accomplished in 1 hour or less. The optimum dose will be determined experimentally. Thermal processing will follow the $^{19}\text{F}^+$ implantation to improve the material sheet resistance and thus the photovoltaic properties. Other possible ions of interest include $^{16}\text{O}^+$, $^{35}\text{Cl}^+$ and $^{58}\text{Ni}^+$. However, these ions are more likely to be investigated in a continuation study rather than during the present one. Also, the effects of pulsed electron beam annealing will be more thoroughly investigated in a future phase of this program.

2.3 MATERIAL EVALUATIONS

Several analytical techniques are available to evaluate the implantation-modified cells and material. The AM0 I-V curves are obtained routinely, and in conjunction with spectral response measurements some clues are obtained about the chemical and physical properties of the material. It is necessary to know the band-gap of the material, which is calculated from the transmittance versus wavelength measurements made on our material units. The calculations are based on methods reported in the literature.⁽³⁾ Table 2 indicates the equation used; the bandgap is obtained by extrapolation of the flat portion of the curve.⁽⁴⁾ A value of 1.1 eV is obtained, the same as for single-crystal silicon. However, by plotting the absorption coefficient, α , versus $h\nu$ for our material, one can observe the strongly improved light absorption characteristics of our material (Figure 9). It is reasoned that better photovoltaic properties are possible with this material.

Infrared absorption spectroscopy has been established as a tool to identify and characterize hydrogenated amorphous silicon. The various Si-H bonds can thus be determined. Several samples were examined with a Fourier-transform infrared spectrometer, and the spectra of three are shown here (see Figures 10, 11 and 12). The first one, Figure 10, shows a number of peaks between 1200 and 2400 wavenumbers. No amorphizing type of implant was used, and consequently peaks characteristic of Si-H bonding in crystalline Si appear; that is, the peaks at 2360 , 2330 , 2130 and 1975 cm^{-1} are

TABLE 2. ABSORPTION COEFFICIENTS FOR α -Si

| Material unit | B-11: $1.3 \times 10^{17} \text{ H}^+/\text{cm}^2$, 50 keV | | |
|---------------|---|---------------------------|--------------------|
| h ν (nm) | Transmittance | $\alpha (\text{cm}^{-1})$ | $h\nu$ |
| 650 | 0.003 | 1.27×10^5 | 4.81×10^2 |
| 750 | 0.036 | 6.53×10^4 | 3.28×10^2 |
| 850 | 0.121 | 3.5×10^4 | 2.26×10^2 |
| 950 | 0.217 | 2.04×10^4 | 1.63×10^2 |
| 1050 | 0.263 | 1.46×10^4 | 1.31×10^2 |

Brodsky et al., "I.R + Raman Spectra ...", Phys. Rev. B 16(8), 3558 (15 Oct. 1977).

$$T = \frac{4T_o e^{-\alpha d}}{(1 + T_o)^2 - (1 - T_o)^2 e^{-2\alpha d}}$$

T = transmittance

$$T_{\Omega} = 0.54$$

α = absorption coefficient

$$d = 4 \times 10^{-5} \text{ cm.}$$

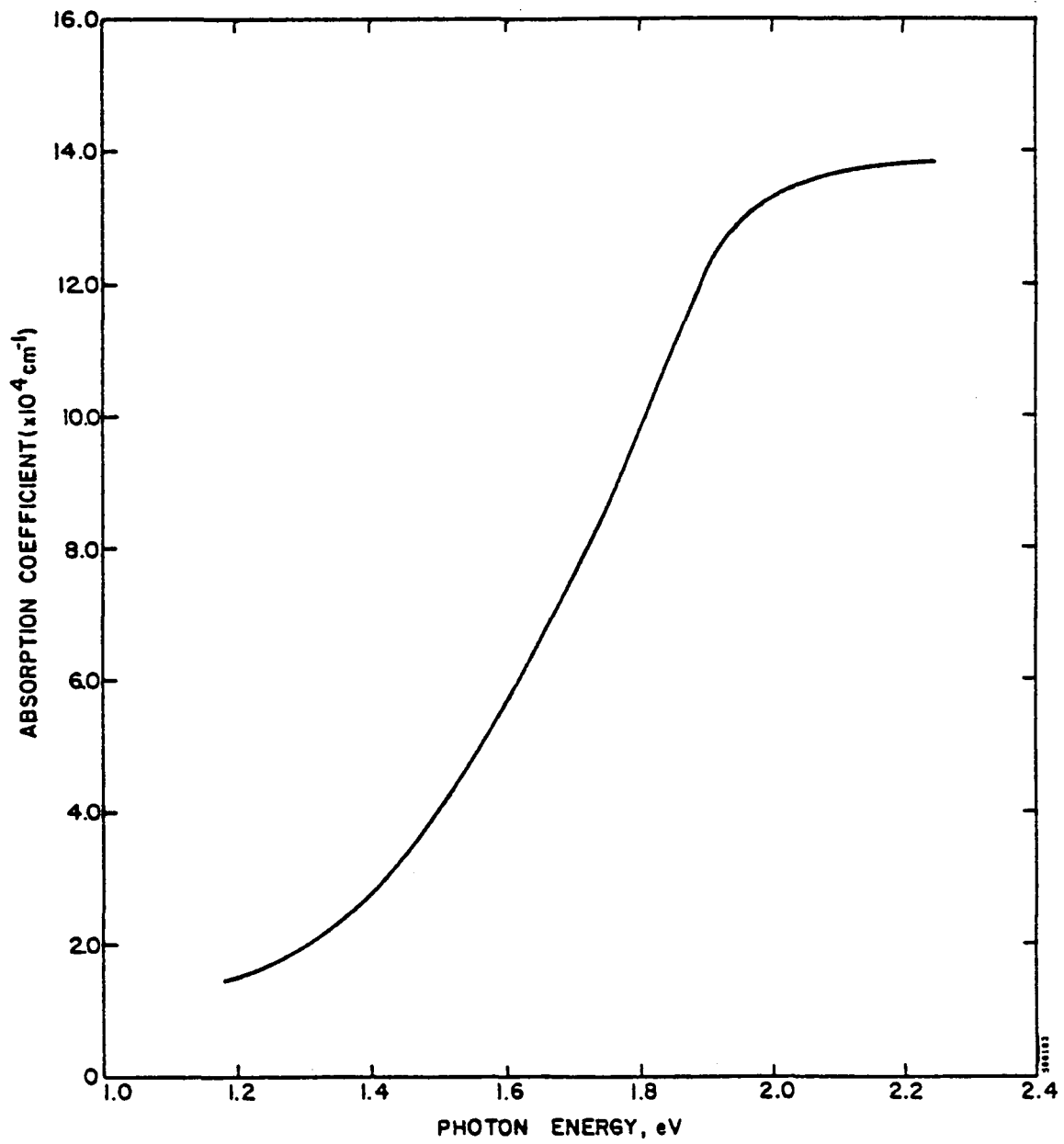


FIGURE 9. ABSORPTION COEFFICIENT FOR MATERIAL UNIT B-11 AFTER Si^+ IMPLANTATION

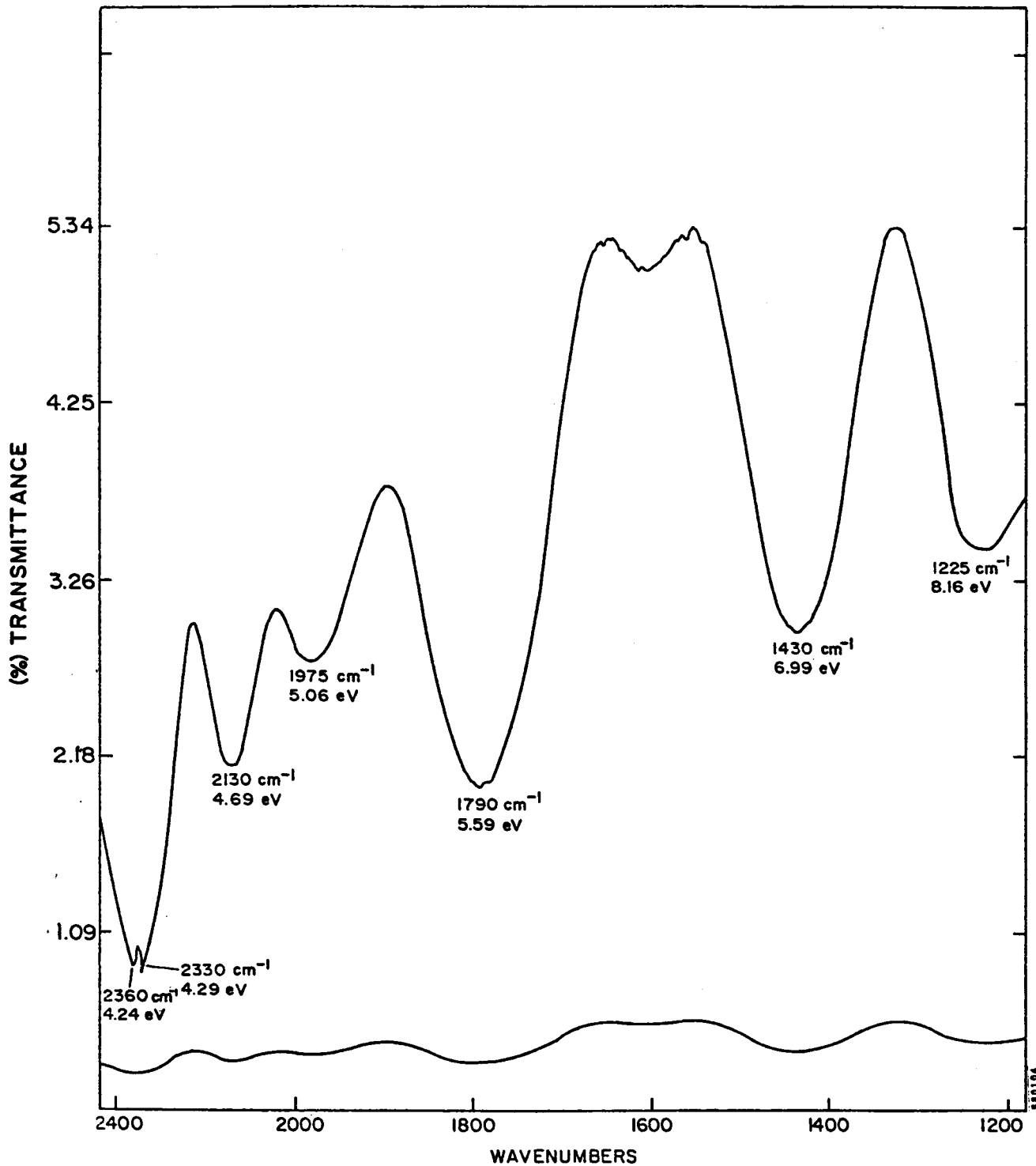


FIGURE 10. INFRARED ABSORPTION SPECTRUM FOR DEVICE UNIT NO. 2191-13

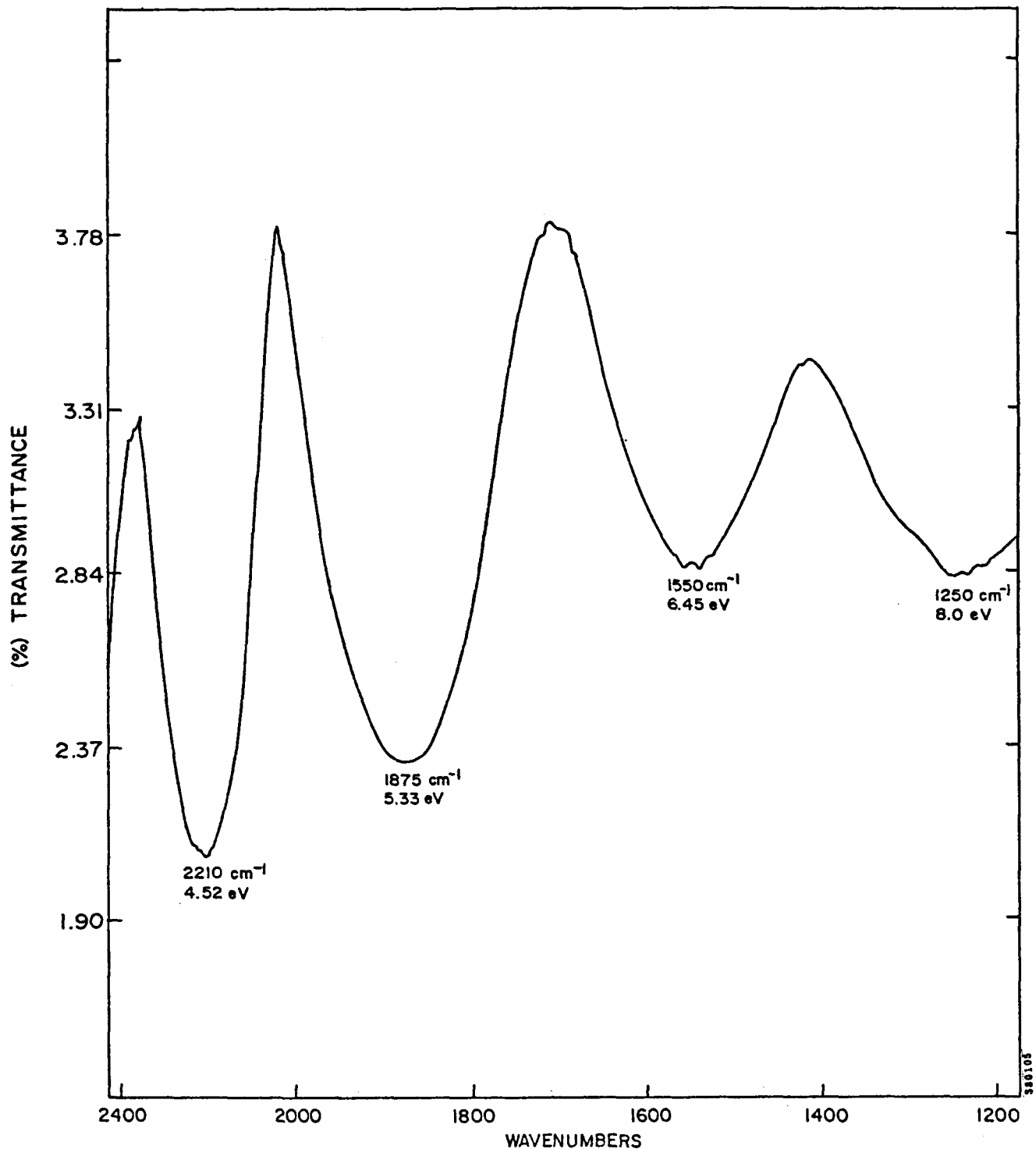


FIGURE 11. INFRARED ABSORPTION SPECTRUM FOR DEVICE UNIT NO. 2150-19
AFTER:

1. $3 \times 10^{15}/\text{cm}^2$ $^{28}\text{Si}^+$ IMPLANT
2. $5.3 \times 10^{17}/\text{cm}^2$ $^1\text{H}^+$ IMPLANT
3. 24 HR ANNEAL AT 250°C
4. 30 MIN ANNEAL AT 300°C

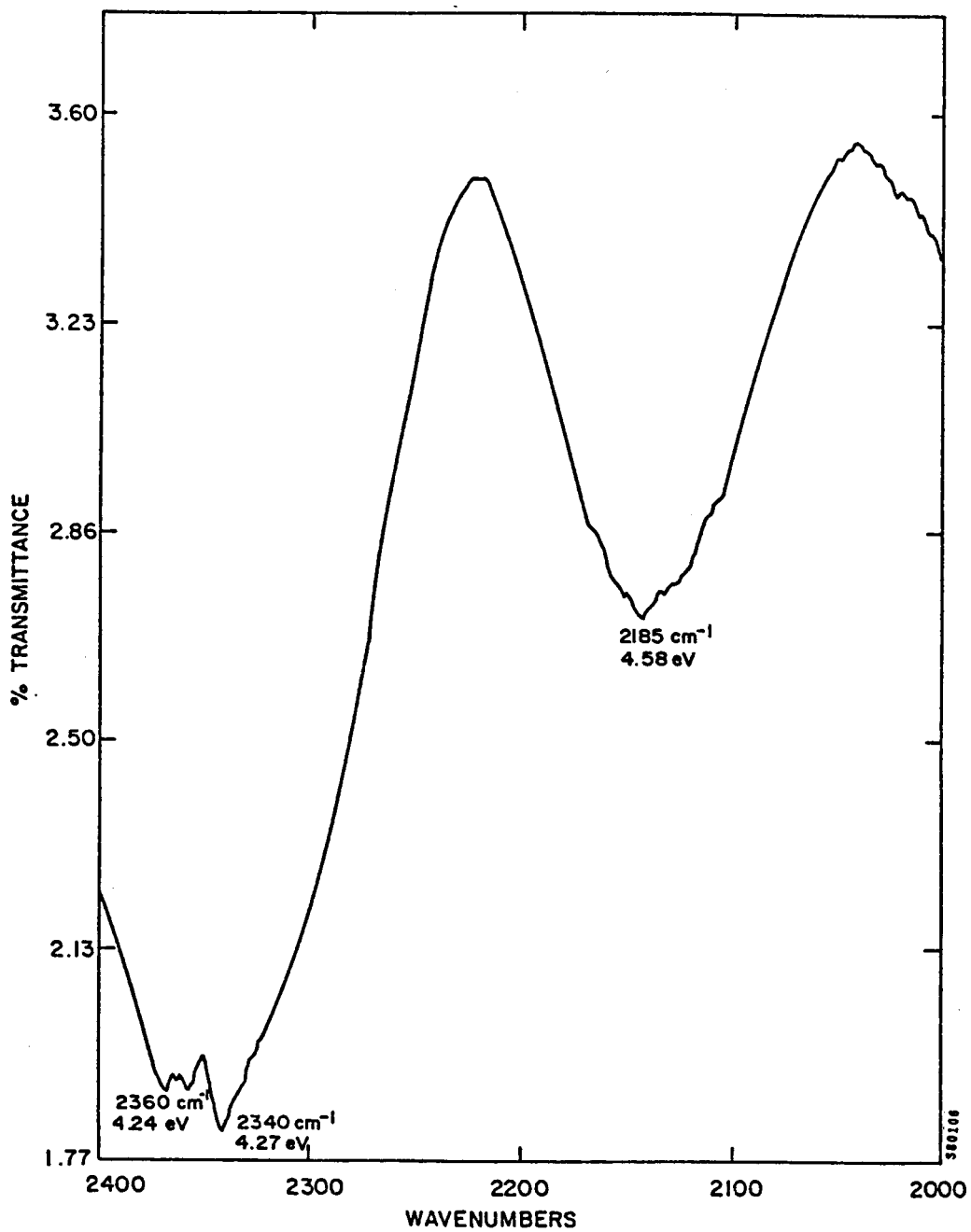


FIGURE 12. INFRARED ABSORPTION SPECTRUM FOR MATERIAL UNIT NO. B-11
AFTER $^{28}\text{Si}^+$ IMPLANT ($8 \times 10^{15}/\text{cm}^2$) AND $5 \times 10^{17} \text{ }^1\text{H}^+/\text{cm}^2$ IMPLANT

typical in this respect. Since only four such peaks appear, as compared to seven reported by H. J. Stein, one may infer that partial annealing has taken place during implantation.⁽⁵⁾ Figure 11 shows a device unit which was Si⁺- and H⁺-implanted and thermally annealed. This time only one peak appears, at 2210 cm⁻¹, which can be attributed to Si-H bonding. One may consider this peak the result of coalescing all the crystalline type of Si-H peaks.⁽⁵⁾ A similar result is shown in Figure 12, which was Si⁺-implanted at a low beam current and had multiple-energy H⁺-implants but no thermal processing. Again one peak appears at 2185 cm⁻¹, but with twin peaks at around 2350 cm⁻¹. One may conclude that both amorphous and crystalline Si-H is seen by the infrared beam. This is explained by geometric considerations in the implantation of the device, which were subsequently corrected. In general the behavior of these units is similar to crystalline or amorphous hydrogenated Si and chemical bonding is possible by implantation alone or followed by thermal processing.

X-ray diffraction spectroscopy can provide useful information on amorphous materials. The degree of disorder and fictive particle sizes can be obtained directly from the diffraction peaks. However, our material is only 0.5 micron thick, at which thickness amorphism is normally difficult to detect by this method. Another method which is more sensitive to thin, surface films is Rutherford backscattering spectroscopy, which by means of ion beam channeling one can easily obtain the degree of disorder. This method is under active consideration. A third method sensitive to amorphous films is reflection high-energy electron diffraction (RHEED), which is also under active consideration. All of the above techniques are routinely available to Spire through its affiliation with the Department of Electrical Engineering at the California Institute of Technology and other laboratories. During the next period we will be using these techniques and reporting on the results obtained.

SECTION 3 SUMMARY

During the third quarter of this program a large number of implantation matrices were evaluated and material investigations initiated. The usefulness of ion implantation in the amorphization and hydrogenation of devices was established. Indeed both of these processes can controllably and reproducibly be carried out. The amorphized material shows superior visible-light absorption behavior compared to crystalline silicon. Hydrogenation with subsequent furnace annealing produces higher open-circuit voltage, in selected devices, than the polycrystalline material. The use of infrared spectroscopy established the presence and type of silicon-hydrogen bonding.

The implantation experiments will continue during the final quarter of this program, with the aim of optimizing the performance of hydrogenated amorphous silicon solar cells by ion implantation.

REFERENCES

1. L. Csepregi et al., *Appl. Phys. Lett.* 29(2) (1976).
2. W. W. Kruehler et al., *Abst. 8th Int. Conf. Amorph. Liq. Semicon.*, Cambridge, Mass. (1979).
3. M. H. Brodsky et al., *Phys. Rev. B* 16(8), 3558 (1975).
4. C. Tsai and H. Fritzche, *Solar Energy Mat.* 1, 29 (1979).
5. H. J. Stein, *J. Electron. Mater.*, 4(1), 159 (1975).
6. H. J. Stein and P. S. Peercy, *Appl. Phys. Lett.* 34(9) (1979).